Influence of temperature and pH on the quality of metastable iron phases produced in zinc-rich solutions

J.O. Claassen[a] and R.F. Sandenbergh[a]

[a]Department of Materials Science and Metallurgical Engineering, **University of Pretoria**, Pretoria, 0002, South Africa

Abstract

The hydrolysis of ferric iron at elevated temperatures and pH values between 1.5 and 3.5 was characterized by determining the stability regions for schwertmannite, 6-line ferrihydrite and 2-line ferrihydrite, and linking them to the supersaturation levels present during their formation. It was shown that most industrial iron removal processes are operated above the metastability limit. However, stagewise precipitation of iron, even above the metastability limit, yielded better quality precipitates. Furthermore, careful selection and control of pH and temperature are required to improve product quality expressed in terms of the solids impurity content, dry solids density, particle size and the particle number density.

Article Outline

1. Introduction

Bulk crystallization processes are widely used in the chemical industry (production of pharmaceuticals to metallic products) to remove wanted and unwanted elements from leach solutions. In hydrometallurgical zinc circuits for example, elements such as iron, cobalt, cadmium, nickel, calcium, copper and lead are all removed in a series of complex precipitation (reaction crystallization), cementation (reduction crystallization) and crystallization processes (cooling crystallization). Even the electroplating process in these zinc-refining circuits may be regarded as a crystallization process, since it requires the same primary and secondary crystallization steps as those encountered in other crystallization processes. The precipitate quality, expressed in terms of particle size and size distribution, impurity content and solids density, generally influences the economics of an operation as it directly impacts on the cost of down stream processing, loss of pay metals in residue streams and the production of a final product that meets client expectations. Gösele et al. (1990) indicated that if crystallization processes are not well controlled, gelatinous and voluminous products are formed which typically have a detrimental effect on down stream processes, such as liquid–solid separation processes, as illustrated in Fig. 1.

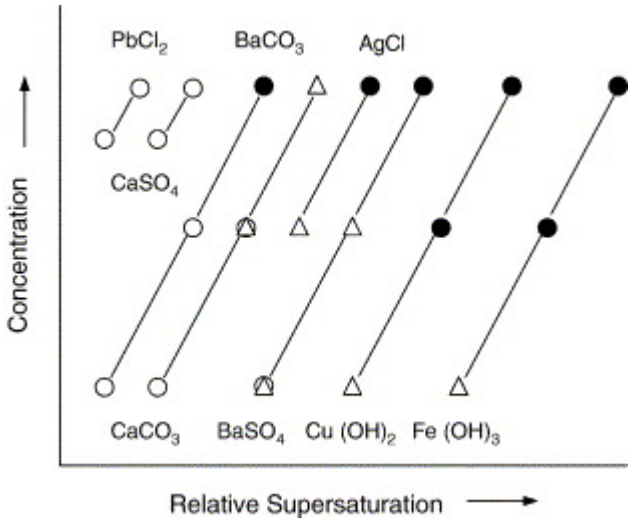

Fig. 1. Simplified diagram of precipitation characteristics of various inorganic salts (after **Gösele et al., 1990**). ○ = crystalline product, ⧋ = temporary gelatinous, ● = permanent gelatinous.

It follows from Fig. 1 that control over the supersaturation and solute concentration is required to ensure the production of a product with adequate down stream processing potential. This is not a straightforward task, especially when poorly soluble phases such as ferric iron hydroxides, are produced. Changes in the operating variables, which include temperature, pH and reduction–oxidation potential supply the driving force, in the form of supersaturation, to crystallization processes and control the solute concentration. These changes not only influence the rate of the primary crystallization steps, i.e. nucleation and growth, but in some instances such as for reaction crystallization processes, it also influences the type of mineralogical phase that is produced and its stability. This is specifically the case when iron is precipitated from hot, dilute solutions where dilution is required to lower the solute iron concentration and improve crystallinity of the final product. By varying the pH and temperature, a series of products in the form of different mineralogical phases with different morphologies, particle sizes, size distributions and densities are produced. The different iron phases that could be produced in a sulphate-containing environment by varying the pH and temperature, as suggested by Babcan (1971), are shown in Fig. 2.

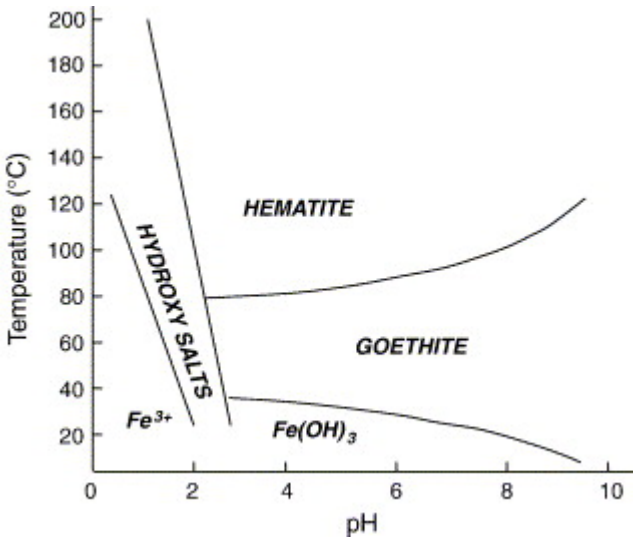

Fig. 2. Phase diagram showing the conditions for the precipitation of different iron phases from 0.5 M ferric sulphate solutions (**Babcan, 1971**). Hydroxy salts = basic iron sulphates. $Fe(OH)_3$ = iron oxy-hydroxide(s).

The iron phases shown in Fig. 2 are not always present in industrial iron residues or residues that contain large amounts of iron. In some environments, it was shown that phases such as ferrihydrite (Jambor and Dutrizac, 1998 and Loan et al., 2001) and schwertmannite (Claassen et al., 2002), which are metastable towards goethite, are produced. Furthermore, the morphologies of these metastable phases differ considerably from each other (Claassen et al., 2002) and from that of goethite.

As was mentioned earlier, temperature and pH not only define the stability of iron phases, as illustrated in Fig. 2, but also impact on the kinetics of the precipitation process, due to their influence on supersaturation. The level of supersaturation, and specifically the critical supersaturation, is described by the so-called metastability curve or metastability limit. The metastable zone, which is the region between the solubility curve and the metastability limit, exists due to the activation energy required to form new particles and defines the supersaturation that might be present when no new nuclei is formed. Within this zone, particle growth in the form of molecular growth is favoured. This results in fewer, bigger, denser particles of a uniform size, whereas above the metastability limit, homogeneous nucleation and agglomeration growth are the dominant processes (Dirksen

and Ring, 1991 and Kind, 2002). This also influences the final product quality since agglomerated particles tend to have much larger surface areas.

Therefore, in order to optimize product quality, specifically in reaction crystallization processes, not only the type of species formed and its stability need to be considered, but also the role that supersaturation plays due to its effect on the primary crystallization processes. In the case of iron precipitates, variables such as pH and temperature determine both the supersaturation and the stability of the species precipitated.

In this paper, special attention is given to the influence of temperature and pH on the stability of ferrihydrite and schwertmannite, the range of the experimentally determined metastable zone compared with the theoretical metastable zone, product quality parameters and the relative supersaturation. The need for this study stems from the fact that very little is published on iron precipitate product quality. Reference is made in the literature to iron precipitate product quality parameters, such as particle size, size distribution and porosity (Cornell and Schwertmann, 1996), but little attention is paid to the factors that influence product quality and the importance of controlling the supersaturation to obtain the desired product (Demopoulos, 1993). This is in sharp contrast to other more simple crystallization systems, which are well described (Nielsen, 1964, Nielsen, 1967, Mullin, 1972, Nyvlt, 1982, Nyvlt et al., 1985, Mersmann, 2001 and David and Klein, 2001).

Furthermore, the (meta)stability, occurrences and properties of ferrihydrite and schwertmannite were established mainly for natural environments (Brady et al., 1986, Bigham et al., 1990, Bigham et al., 1994, Bigham et al., 1996 and Jambor and Dutrizac, 1998), whereas this study focuses on the hydrolysis of ferric iron at elevated temperatures in a zinc sulphate environment.

2. Experimental

The experimental work performed comprised three parts. The first part of the study focused on the determination of the metastability limit and the relative supersaturation

levels, followed by an investigation into the benefits of stagewise precipitation. Lastly, information was gathered on the influence of specifically temperature and pH on some product quality parameters.

2.1. Determination of phase stability regions

The experimental arrangement consisted of a sealed, flat-bottomed stirred tank reactor with a diameter (D) of 120 mm and working volume of 2 L, equipped with four outer baffles. It was stirred with a three-blade marine-type impeller with diameter $d \sim D / 2$ rotating at 1000 rpm. The temperature was controlled within 1 °C of the setpoint using a heating mantle and controller.

Experiments were conducted at temperatures of 50, 70 and 90 °C and at pH values ranging from 1.5 to 3.5. The pH was measured at temperature (automatically compensated for by the instrument). For each experiment, a solution containing 5 g/L sulphuric acid and about 11.5 g/L Fe as $Fe_2(SO_4)_3$ was prepared. The pH was raised manually at a rate of approximately 0.5 units every 20 min on the forward cycle using $Ca(OH)_2$ powder (pH range 1.5 to 2.5) and ZnO powder (pH range 2.5 to 3.5). On the reverse cycle (pH 3.5 to pH 1.5), 98% sulphuric acid was added drop wise to lower the pH at the same rate mentioned above. Each experiment was repeated at least three times. Samples were taken at regular pH intervals, except over the critical pH range, where the critical supersaturation level was exceeded, where samples were taken more frequently. Approximately 10 mL solution was extracted during the sampling process. Each sample was immediately filtered using Whatman Grade 542 paper and the extracted solution was analysed for ferric iron concentration and pH. Distilled water and chemicals of CP grade were used in all experiments.

2.2. Stagewise precipitation

The experimental setup used comprised three crystallizers in series, each with an active volume of 3.96 L and an inside diameter of 16 cm. Each reactor was equipped with four outer baffles fixed to the wall of the vessel, a riser box and overflow launder, as shown in Fig. 3.

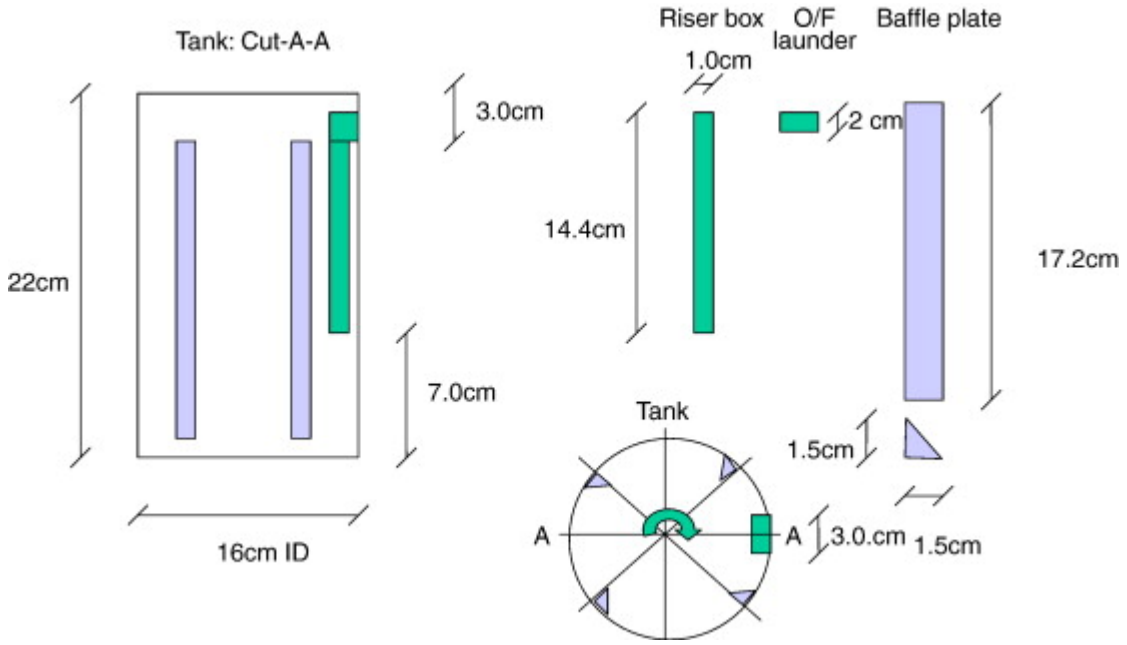

Fig. 3. Dimensions of the crystallizer used to determine the influence of stagewise precipitation on product quality.

Three-blade marine type impellers, with diameters $d \sim D$ / 2.5, were used at a stirring rate of 600 rpm to keep the solids in suspension. The hot iron solution contained 5 g/L free acid and 15 g/L iron, added as $Fe_2(SO_4)_3$. Roasted zinc calcine, in the form of a 7.5% calcine slurry prepared with distilled water, was used as neutralising agent. The calcine used had a d_{50} value of about 38 µm and ZnO content of approximately 70%. In all experiments the calcine slurry and hot iron solution were pumped continuously to the first of three reactors in series to control the pH at the predetermined setpoints. The two streams were placed on opposite sides of the reactor with the outlet points positioned just below the agitator blades. Hot iron solution and ZnO slurry was also pumped on separate lines to reactors 2 (Experiments 1 and 2) and 3 (Experiment 3) respectively to adjust the pH values as indicated in Table 1.

Table 1.

Experimental conditions used to determine the influence of stagewise precipitation on product quality

Experiment	**Parameters**		**Flows**	
	Temperature (°C)	**pH profile**	**Iron solution (mL/min)**	**Calcine slurry (mL/min)**
Base case	65	3.20	26.9	41.1
		3.31		
		3.39		
1	65	3.20	26.9	41.1
		2.80	1.33	
		2.94		
2	65	2.50	29.0	36.1
		3.00		2.5
		3.09		
3	65	2.50	26.9	45.0
		2.74		
		3.01		0.8

Samples of 250 mL each were taken from reactor 3 at the end of each experiment, which lasted for about 3 h, and immediately filtered using Whatman Grade 542 paper. The solution samples were analysed for pH and ferric iron concentration. The filter cakes were weighed and dried to determine the moisture content and analysed for zinc and iron. The dry solids density of each sample was also determined using a water displacement method. Wet filter cake samples were taken and mixed with distilled water to determine particle size and size distribution using a Malvern particle size analyser.

2.3. Determination of the influence of temperature and pH on product quality

In order to determine the influence of pH and temperature on product quality parameters such as cake moisture content, particle solids density, particle impurity content (zinc and sulphate) and particle size, the sealed glass precipitator with an active volume of 2 L, mentioned earlier, was used in a continuous mode. Hot iron solution containing 5 g/L free acid and 10 g/L iron, added as $Fe_2(SO_4)_3$, as well as a 2.5% ZnO slurry were continuously pumped to the reactor using peristaltic pumps. All the reagents used were of CP grade. The outlet points of the reactant streams were placed just below the agitator blades on opposite sides of the vessel. The level in the reactor was controlled with another peristaltic pump. The flow rate of ZnO slurry varied with a change in the pH setpoint as summarized in Table 2.

Table 2.

Average hot iron solution (HIS) and ZnO slurry flow rates used to precipitate iron at different pH setpoints

pH	HIS flow rate (mL/min)	ZnO slurry flow rate (mL/min)
1.8	21.1	< 1
2.2	21.1	10
2.6	21.1	14
3.0	21.1	16
3.4	21.1	17

Experiments were performed at temperatures of 50, 60, 70 and 80 °C. Each experiment ran for 3 h and was repeated at least three times. At the end of each experiment, two 250 mL samples were taken. The first sample was filtered using Whatman Grade 542 paper and dried at 120 °C for 1 h to determine the cake moisture content. The other sample was filtered and the cake washed with 1 L of hot water. The filtrate extracted prior to the hot water wash, was analysed for ferric iron and pH. The washed filter cake was again dried at 120 °C for 1 h, analysed for zinc and sulphate and the dry solids density determined. The dry solids density was determined using a water displacement

method. Wet filter cake samples of about 5 mL each were also taken and mixed with distilled water at ambient temperature to determine the product mean particle size and size distribution using a Malvern particle size analyser.

XRD analyses were performed on the dried, washed filter cake. Cu-Kα radiation at a wavelength of approximately 0.154 nm was used.

3. Results and discussion

3.1. The role of the supersaturation level in iron precipitate product quality

3.1.1. Determination of the metastability limit and metastable zone width

In order to develop a (meta)stability diagram for iron precipitated from a ferric iron solution under industrial conditions and to calculate typical supersaturation levels present during this process, the metastability zone for iron precipitation had to be determined first. This was done using a method of cycling the pH between a lower and higher limit at different temperatures. The ferric iron concentration as a function of pH at a specific temperature was then plotted, as shown in Fig. 4. The critical pH values for nucleation (A) and solubilization (B) were then determined by extrapolation of the slope of the ferric concentration versus pH line to the initial ferric concentration.

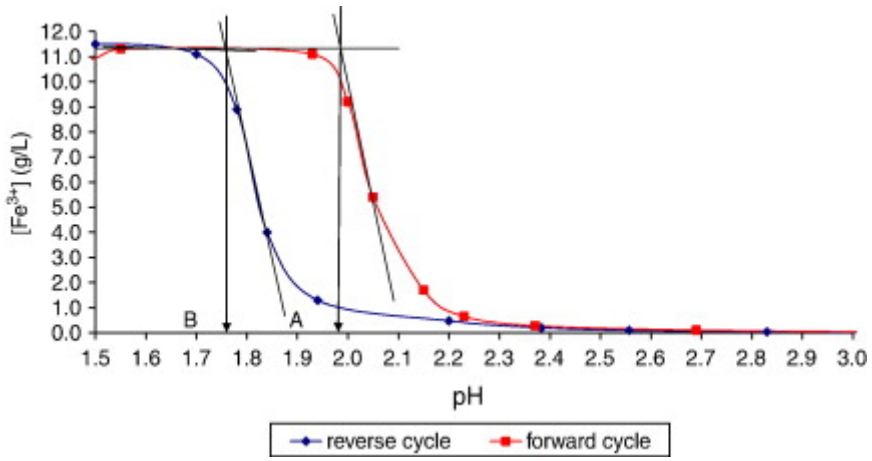

Fig. 4. Average ferric iron concentration as a function of pH determined at 50 °C. The pH was changed stepwise in increments of 0.5 pH units every 20 min. The pH was increased by adding $Ca(OH)_2$ and ZnO powder and decreased by adding 98% H_2SO_4.

From the data presented in Fig. 4, the critical pH values of nucleation (point A, pH ≈ 1.97) and solubilization (point B, pH ≈ 1.76) were determined. The critical pH values for nucleation and solubilization, defining the boundaries of the metastable zone, are shown in Fig. 5.

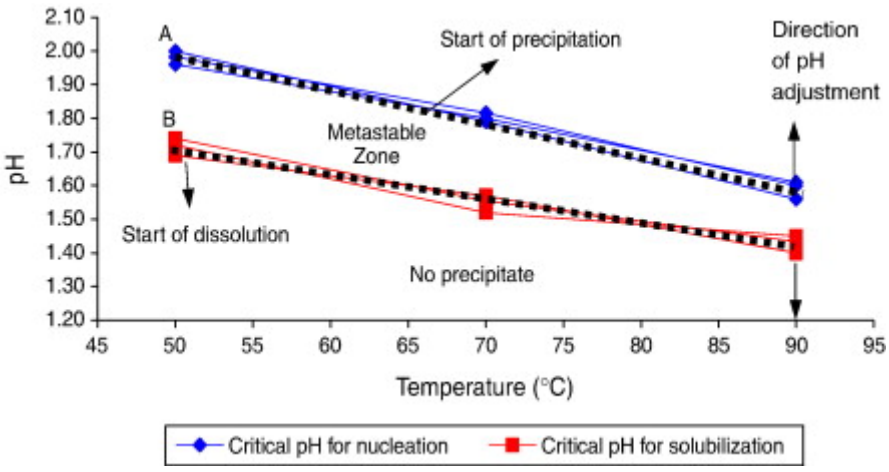

Fig. 5. Illustration of the metastable zone width determined for the precipitation of iron from a ferric iron solution containing approximately 11.5 g/L Fe added as $Fe_2(SO_4)_3$ and 5 g/L H_2SO_4. The pH was varied using $Ca(OH)_2$ and ZnO powder and 98% H_2SO_4.

According to the definition of the metastable zone, the equilibrium solubility limit forms the lower boundary of the metastable region. However, the width of the metastable region may be reduced by an increase in temperature, the presence of isomorphic and anisomorphic material (Garside et al., 1972 and Mullin and Ang, 1976) and a mixing intensity such as the 1000 rpm used. When the solubility limit determined in this study (Fig. 5) is compared with the equilibrium solubility limit, the reduction in the width of the metastable zone is evident as shown in Fig. 6. STABCAL™ software with the MINTEQA2 database was used to calculate the equilibrium [Fe^{3+}] solubility line *X* (ΔG_f $HFeO_2$ = − 468.607 kJ/mole at 50 °C) and the data for line *Y* was taken from the literature (Cornell and Schwertmann, 1996). Lines *X* and *Y* show the equilibrium solubility of goethite, which is the equilibrium phase for ferrihydrite and schwertmannite, respectively as a function of pH. Line *Z* indicates the spontaneous precipitation limit for ferrihydrite as calculated with the same database. In this study, iron concentrations reflected by the

experimental forward cycle line and line *Y* were used to calculate the relative supersaturation present during iron precipitation, as will be shown later.

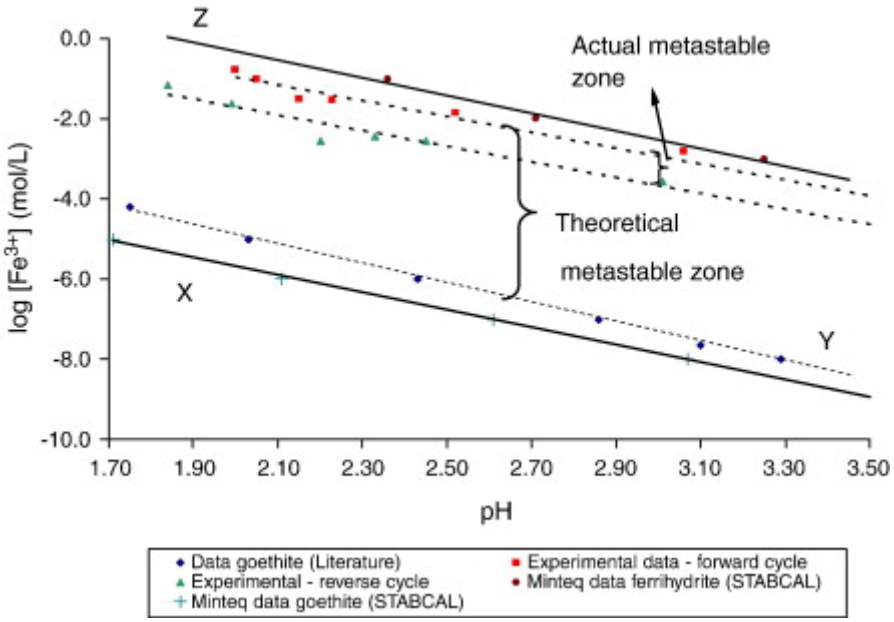

Fig. 6. Ferric concentration as a function of pH for the precipitation of iron at 50 °C from a ferric iron solution containing approximately 11.5 g/L Fe added as $Fe_2(SO_4)_3$ and 5 g/L H_2SO_4. The pH was varied using $Ca(OH)_2$ and ZnO powder and 98% H_2SO_4. The experimental reverse cycle line forms the new solubility limit.

It follows from Fig. 6 that a high degree of supersaturation is required to initiate precipitation and that the relatively narrow metastable zone of between 0.2 and 0.3 pH units (from Fig. 5), would require precise control to achieve good precipitate properties. Precipitation from highly supersaturated solutions, which is more often than not the case in iron precipitation processes (Claassen et al., 2003), will result in the rapid nucleation of very fine crystals which subsequently aggregate to form larger particles. (Dirksen and Ring, 1991). Furthermore, the choice to utilise the metastability limit to improve product quality is influenced by factors such as the co-precipitation of other phases, i.e. phases resulting from the presence of silica in some industrial hot iron solutions, the value of the product being removed, as recycling has a cost implication, the reduction in the concentration of oxygen or gaseous reagents at low pH values (goethite iron removal process) and the need to precipitate a specific iron phase, such as ferrihydrite, that is stable only at higher pH values.

Therefore, although the metastable zone might be useful in the chemical industry, i.e. in the production of pigments, the factors listed above should be considered in metallurgical processes. It nonetheless, provides useful information that could be used to improve product quality in some iron removal processes. Firstly, it could act as a control reference point to lower supersaturation in an iron precipitation process and/or it could be used to calculate typical supersaturation levels in a specific application, as illustrated in the following paragraphs. Secondly, it could be used to illustrate why stagewise precipitation (Demopoulos, 2003) could improve iron precipitate product quality. Generally, the solute concentration changes stepwise with a step change in temperature (cooling crystallization) or pH (reaction crystallization) within the metastable region. By using the same principle, even at conditions outside the metastable zone, it was shown that product quality could be improved as discussed later in the paper.

3.1.2. Determination of phase stability regions

The relative supersaturation present during a precipitation process typically determines the quality of the precipitate, with poorer quality precipitates being formed at higher levels of supersaturation. The relative supersaturation (σ) present during the precipitation experiments was calculated using the minimum concentration required to initiate precipitation substituted in Eq. (1), and shown in Fig. 7 as a function of pH and temperature.

$$\sigma=(c-c_{eq})/c_{eq}=\Delta c/c_{eq} \quad (1)$$

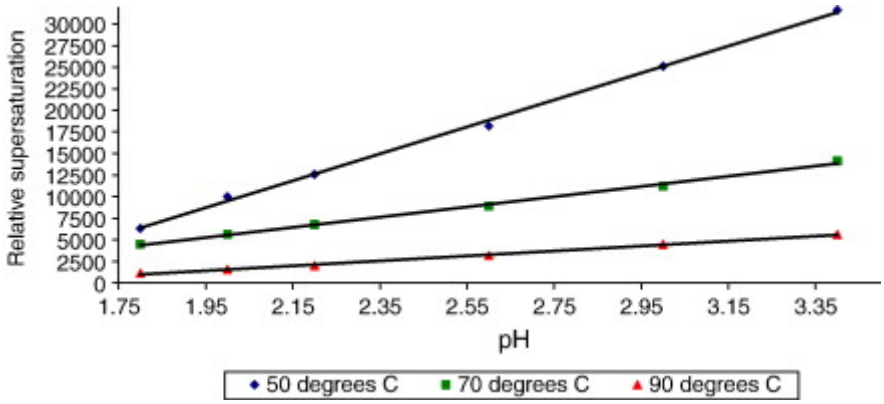

Fig. 7. Calculated minimum relative supersaturation as a function of pH at different temperatures for the hydrolysis of ferric iron from iron solutions containing approximately 11.5 g/L Fe added as $Fe_2(SO_4)_3$ using $Ca(OH)_2$ and ZnO powder to control the pH.

Where:

c

actual solute concentration (mol/L)

c_{eq}

equilibrium solute concentration (mol/L)

From Fig. 7 it is clear that lower degrees of supersaturation are required for precipitation of iron at higher temperatures and lower pH values. Better quality precipitates could thus be expected for such conditions. This was indeed found to be the case in previous work (Claassen et al., 2002) where open structured ferrihydrite was produced at a temperature of 65 °C and a pH of 3.2 compared to more dense schwertmannite obtained at 65 °C and a pH of 2.7, as shown in Fig. 8.

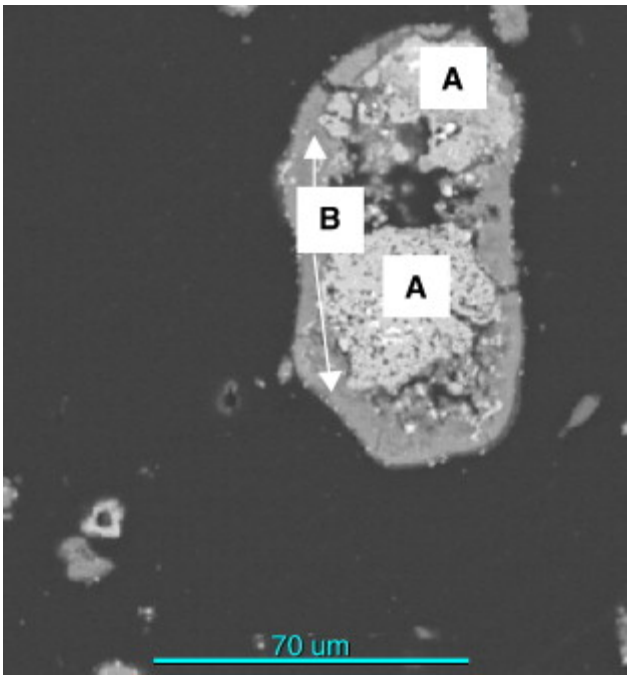

Fig. 8. SEM backscattered image of an iron-bearing particle, showing open structured ferrihydrite particles (Particles A) covered with a more dense structured schwertmannite layer (Portion B) (**Claassen et al., 2002**).

The zones for metastable iron precipitation may be defined in terms of temperature and pH by considering the chemical analyses, in the case of the hydroxy salts, and XRD analyses, in the case of ferrihydrites, and are shown as Fig. 9.

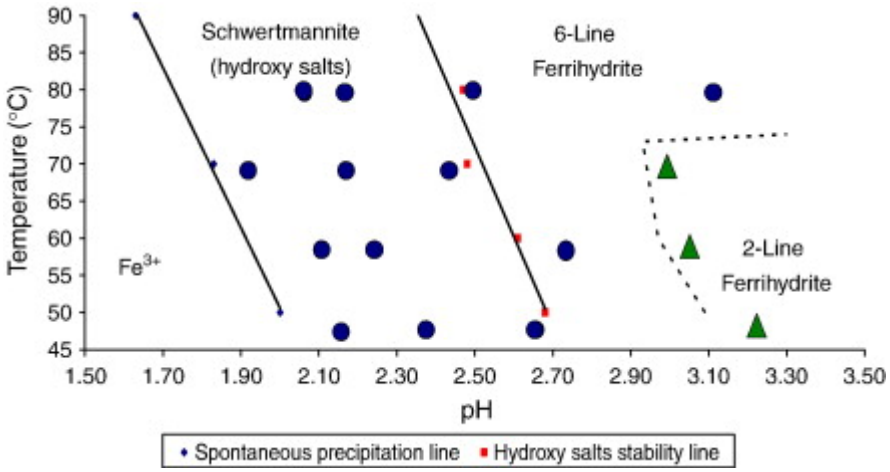

Fig. 9. Metastability diagram for ferric iron hydrolysis from a 10 g/L Fe (added as $Fe_2(SO4)_3$) solution using ZnO powder to control the pH. ● = 6-line ferrihydrite and schwertmannite and ▲= 2-line ferrihydrite obtained from XRD analyses. The total sulphate concentration varied between 0.20 and 0.25 moles/L.

In Fig. 9, the boundary between the hydroxy salts (schwertmannite) and ferrihydrite was obtained by washing the precipitates produced in the continuous reactor with hot water, and noting the conditions where the sulphate content started to rise, as indicated in Fig. 10.

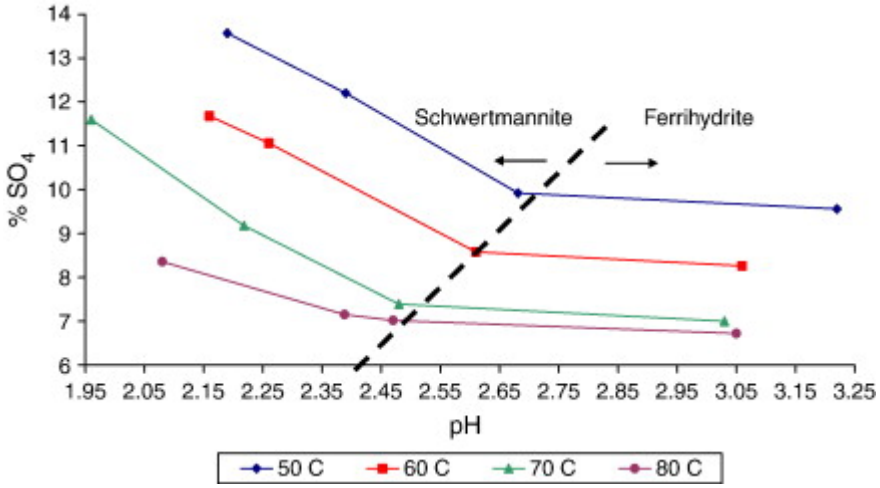

Fig. 10. Influence of pH and temperature on the sulphate content of iron precipitated from a hot iron solution containing 10 g/L Fe (added as $Fe_2(SO_4)_3$) using ZnO powder to control the pH in a continuous reactor.

The different iron phases and their crystallinity were identified using XRD analyses. The data obtained for the 60 °C isoterm are summarized in Table 3.

Table 3.

X-ray diffraction results obtained from synthetic iron precipitate samples produced in a continuous reactor at 60 °C

pH	***d*-values (nm)**		
	Schwertmannite	**2-line ferrihydrite**	**6-line ferrihydrite**
3.06		Uncertain	
		Uncertain	
		0.2561	
		Very weak	
		Very weak	
		0.1506	
		Very weak	
2.75			0.5033[a]
			0.3323[a]
			0.2554
			0.2219
			0.1927
			0.1702
			0.1510
			Very weak
2.16	0.4895		
	0.3423		
	0.2526		
	0.2214		
	0.1940		
	0.1648		
	0.1517		

pH	***d*-values (nm)**		
	Schwertmannite	**2-line ferrihydrite**	**6-line ferrihydrite**
	Very weak		

[a] Indicate presence of schwertmannite.

The data obtained in Table 3 is in good agreement with work done by Bigham et al. (1990), Jambor and Dutrizac (1998) and Claassen et al. (2002).

The determination of the schwertmannite (meta)stability region at elevated temperatures is unique as it has previously only been identified in natural environments (Bigham et al., 1990, Bigham et al., 1994 and Bigham et al., 1996). It also appears from Fig. 10, as if there is a definite hydroxy salt/schwertmannite phase transition line, as indicated in Fig. 9, which supports the notion of schwertmannite as a separate phase, rather than being ferrihydrite with adsorbed sulphate. It appears from Fig. 10 rather as if both ferrihydrite and schwertmannite contain variable amounts of sulphate, which probably result from a change in morphology with a change in pH and temperature and increased stability of ferrihydrite with an increase in pH and temperature above the hydroxy salt stability line. Furthermore, the different slopes shown for the sulphate curves in the schwertmannite region indicated in Fig. 10, probably supports findings that schwertmannite is not a unique mineral but rather a class/series of minerals (Barham, 1997).

If the data in Table 3 is considered, it appears as though schwertmannite is also present at pH values above the hydroxy salt stability line (6-line ferrihydrite region) as indicated by the presence of peaks at approximately 17 and 27 2θ, which are not well defined in the case of ferrihydrite, as shown in Fig. 11.

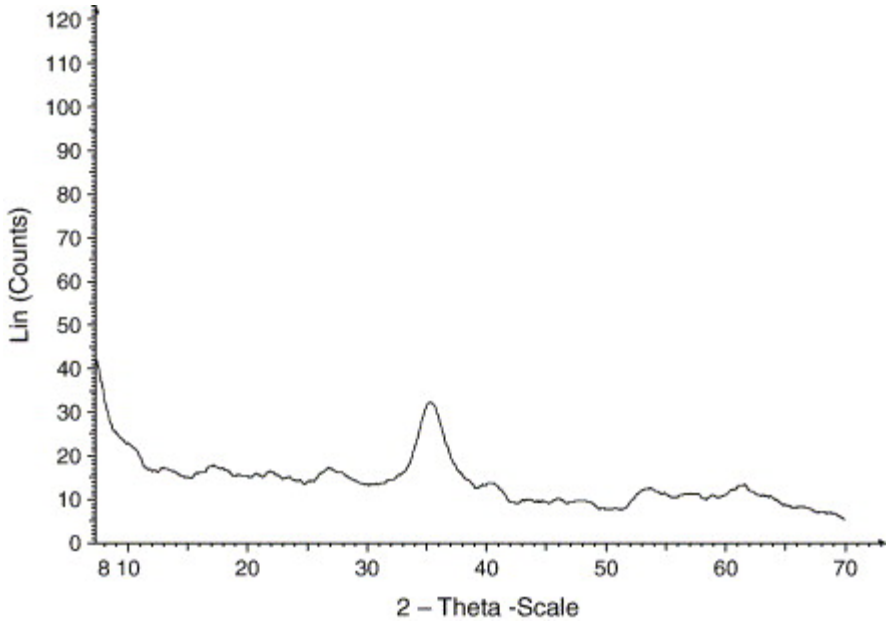

Fig. 11. X-ray diffractogram of a poorly crystalline synthetic iron precipitate produced at 60 °C and a pH of 2.75 in a continuous crystallizer.

The stability of iron hydroxy sulphates in an acidic environment, stems from the presence of species such as $[FeSO_4]^+$ in iron sulphate media, that is believed to play an important role in the formation of these phases (Ashurst and Hancock, 1977). Species such as $Fe_2(OH)_2(SO_4)_2$ were also found in sulphate solutions, which is believed to be the precursors of iron hydroxysulphate precipitates (Yakovlev et al., 1977).

Finally, the influence of supersaturation on the quality of iron phases produced at temperatures between 50 °C and 90 °C and pH values between about 1.5 and 3.5, can be summarized by combining the data presented in Fig. 7 and Fig. 9, as shown in Fig. 12.

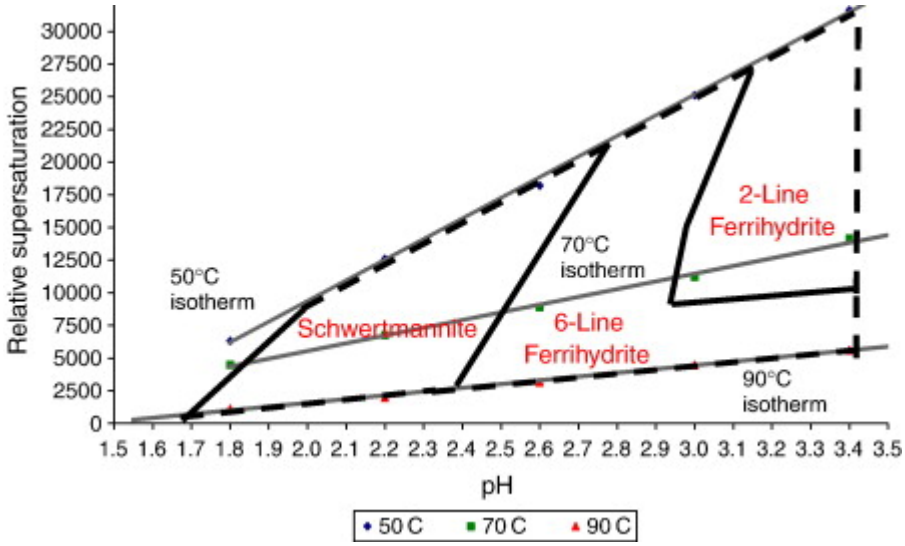

Fig. 12. Phase stability regions of metastable iron phases expressed in terms of relative supersaturation and pH.

From Fig. 12 it is clear that the different precipitates are formed over a range of supersaturations. It can be expected that the best quality precipitates are formed at lower degrees of supersaturation.

3.1.3. Stagewise precipitation

Stagewise precipitation is done by operating within the metastable zone to improve product quality. The applicability of this approach to a process operated above the metastable region was evaluated. Table 4 summarizes the results obtained when iron was removed stagewise using three continuous crystallizers in series.

Table 4.

Results obtained from stagewise iron removal experiments performed at 65 °C

Experiment	pH profile	Cake moisture (%)	Water soluble Zn[a] (%)	Weak acid soluble Zn[b] (%)
Base case	3.20	57	2.86	5.41
	3.31			
	3.39			
1	3.20	54	1.57	3.83
	2.80			
	2.94			
% Improvement		5.3	45.1	29.2
2	2.50	43	1.18	3.65
	3.00			
	3.09			
% Improvement		24.6	58.7	32.5
3	2.50	46	1.22	4.02
	2.74			
	3.01			
% Improvement		19.3	57.3	25.7

[a] Filter cake washed with hot water only to remove water soluble zinc.

[b] Filter cake washed with a pH = 1.5 solution to remove entrapped zinc.

In the base case experiments, hot iron solution was contacted with calcine slurry at a pH of 3.2 in the first of three reactors in series, where after the pH increased without further additions to about 3.4 in the last reactor. According to Fig. 9 and Fig. 12, 2-line ferrihydrite was probably produced at a relatively high relative supersaturation level of about 17,000 in this process. Particles with a high surface area were probably formed,

which would explain the relatively high moisture and impurity content in terms of water soluble and weak acid soluble zinc values of the precipitate as summarized in Table 4. In Experiment 1, an acid wash stage was performed at pH 2.80 in the second reactor. This mode of operation is utilised in the Zincor roast-leach-electrowinning zinc refinery (Claassen et al., 2003) to remove iron from zinc-rich process solutions. During the acid wash step, some 2-line ferrihydrite particles were probably dissolved and reprecipitated as 6-line ferrihydrite and schwertmannite (refer to Fig. 9 and Table 3) at relative supersaturation levels around 15000. This leaching step resulted in a probable reduction in the relative particle surface area as well as the zinc content of the solids formed, as shown in Table 4.

Experiments 2 and 3 were used to investigate the influence of stagewise precipitation on some product quality parameters, i.e. the pH was incrementally increased to remove iron to the desired levels. In Experiment 2, the pH in the first reactor was controlled at 2.5, followed by an increase in pH, through the addition of calcine slurry into the second reactor to raise the pH to 3.0, where after it increased to about 3.1 in the last vessel. In the first reactor schwertmannite, which has a more dense structure than ferrihydrite, was probably produced at relative supersaturation of about 12,000. The lower nucleation rates, at lower supersaturation, and improved leaching of the ZnO neutralising agent probably resulted in a significant reduction in the impurity levels of the final product, as is evident from the data presented in Table 4. The remaining supersaturation was then used in the second reactor to probably agglomerate the particles. In Experiment 3, the pH in the first reactor was again controlled at 2.5, and then left to increase to about 2.75 in the second reactor. Calcine was added to the third reactor to increase the pH to 3.00 to ensure adequate iron removal, which could explain the slight increase in the zinc values of the final product. These results indicate that the stagewise precipitation of iron, even above the metastability limit, could significantly improve product quality.

3.2. The influence of temperature and pH on final product quality

3.2.1. Solids moisture content

The moisture content of a precipitated product could be used to indicate its downstream processing potential in terms of its drying requirements and ease of handling, as it gives an indication of the relative surface area of the precipitates. The precipitate moisture content is significantly influenced by pH and temperature as indicated in Fig. 13. Cake moisture decreases with an increase in temperature and reaches a minimum at pH values between 2.45 (80 °C) and about 2.68 (50 °C). The effect of temperature on precipitate moisture content is probably the result of the formation of more dense particles at higher temperatures as indicated by the results shown in Fig. 14.

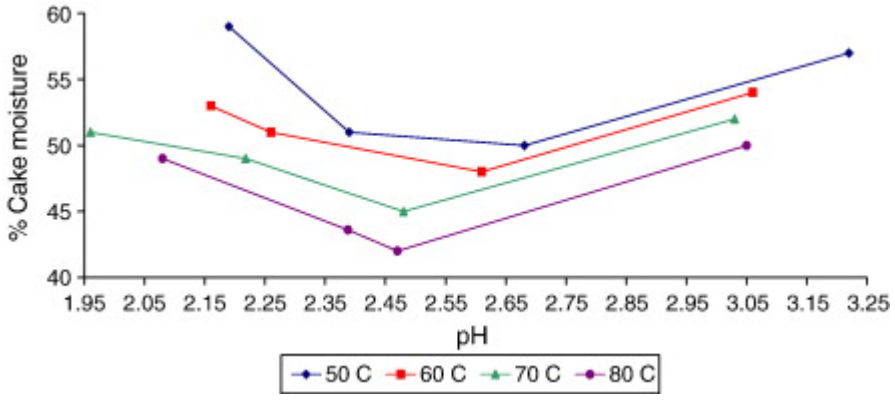

Fig. 13. Filter cake moisture content for iron precipitates produced in a continuous crystallizer from a hot iron solution containing 5 g/L H_2SO_4 and 10 g/L Fe (added as $Fe_2(SO_4)_3$) using ZnO powder as neutralising agent as a function of pH and temperature.

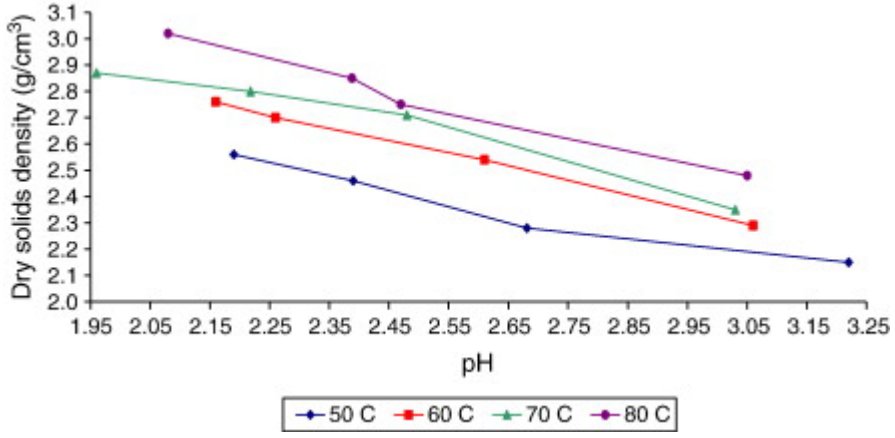

Fig. 14. Influence of pH and temperature on precipitate solids density for iron precipitates produced in a continuous crystallizer from a hot iron solution containing 5 g/L H_2SO_4 and 10 g/L Fe (added as $Fe_2(SO_4)_3$) using ZnO powder as neutralising agent.

It is known that better quality precipitates are formed at higher temperatures as a result of lower supersaturation levels as indicated in Fig. 12. The increase in moisture content at lower and higher pH values is probably a result of a reduction in the mean particle size (increase in relative surface area) at lower pH and the formation of more voluminous particles at higher pH values. The high supersaturation levels generated at high pH values also supports fast nucleation rates and an increase in population density and surface area. Both the mean precipitate particle size (d_{50}) and population density increase with increasing pH, as shown in Fig. 15 and Fig. 16, respectively. The increase in size of the particles is most probably caused by agglomeration.

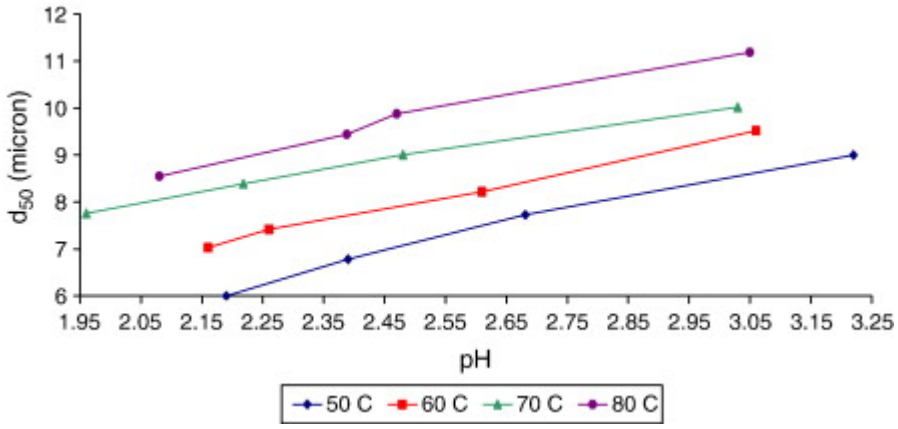

Fig. 15. Influence of pH and temperature on the mean particle size for iron precipitates produced in a continuous crystallizer from a hot iron solution containing 5 g/L H_2SO_4 and 10 g/L Fe (added as $Fe_2(SO_4)_3$) using ZnO powder as neutralising agent.

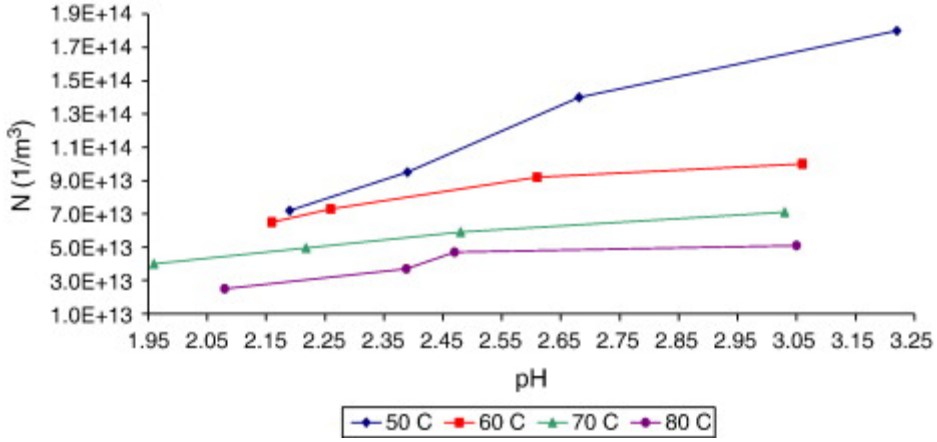

Fig. 16. Influence of pH and temperature on precipitate population density obtained from Malvern particle analyses for iron precipitates produced in a continuous crystallizer from a hot iron solution containing 5 g/L H_2SO_4 and 10 g/L Fe (added as $Fe_2(SO_4)_3$) using ZnO powder as neutralising agent.

3.2.2. Solids impurity content

Reaction crystallization requires a reagent to generate the necessary chemical driving force for solids formation from leach solutions. In the zinc industry, ferric iron is often removed through hydrolysis by contacting hot iron solution with zinc calcine containing approximately 70% ZnO, as summarized by Claassen et al. (2003). The use of a zinc containing neutralising agent typically results in high zinc losses and often the production of iron residues with high sulphate loadings. Fig. 17 shows the influence of pH and temperature on the zinc content of ferric iron precipitated through hydrolysis using ZnO as the neutralising agent. The zinc content of iron precipitates increased significantly with an increase in pH and temperature. This is probably the result of a combination of high supersaturation (at higher pH values) and faster diffusion of iron species to the growth points (Sakamoto et al., 1976 and Yamada, 1980), which could entrain unleached ZnO or zinc sulphate solution. The reduction in the reactivity of ZnO with an increase in pH, probably exacerbated the problem.

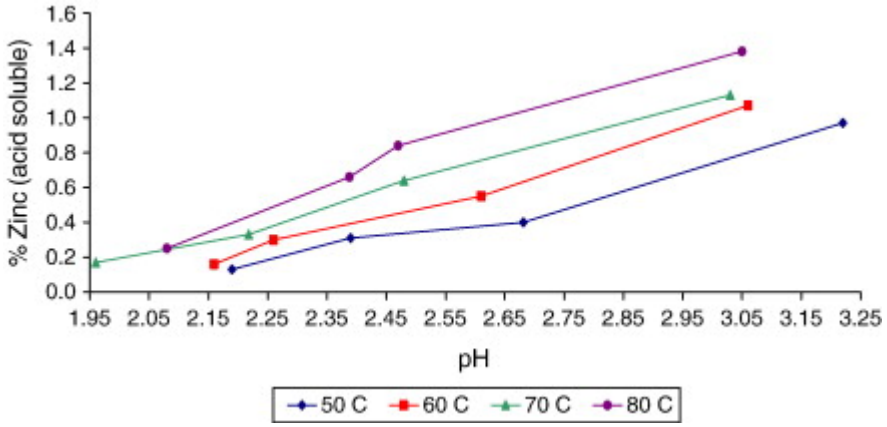

Fig. 17. Influence of pH and temperature on the zinc content of iron precipitates produced in a continuous crystallizer from a hot iron solution containing 5 g/L H_2SO_4 and 10 g/L Fe (added as $Fe_2(SO_4)_3$) using ZnO powder as neutralising agent.

4. Conclusions

Control over the factors that influence product quality in crystallization processes is of utmost importance at it affects the economics and ease of handling in down stream processes. The type of phase produced and the supersaturation mainly influence final product quality. Hydrolysis of ferric iron in the temperature range 50 °C to 90 °C and at pH values between about 1.5 and 3.5, as typically used in many industrial processes, results in the formation of poorly crystalline, metastable iron phases such as ferrihydrite (2-line and 6-line) and schwertmannite. In this study, the stability regions of these phases were determined as a function of easily controllable parameters such as pH and temperature. Typical relative supersaturation levels required for the precipitation of ferrihydrite and schwertmannite were also calculated from spontaneous precipitation data. It was shown that ferrihydrite and schwertmannite are formed over a range of supersaturation levels between about 1000 and 30,000. It appears as though hydroxy salts, which include schwertmannite, are generally of a better quality as indicated by a higher solids density and lower impurity content than oxyhydroxides, which include ferrihydrite, that were formed at higher relative supersaturation, i.e. lower temperatures and higher pH values.

The study showed that even though poorly crystalline iron phases were produced, the quality of these phases could be improved by controlling the supersaturation. This could be done through careful selection and control of parameters such as pH and temperature and using a stagewise precipitation process. Other factors that influence product quality such as the mixing environment and agglomeration were also studied and are discussed elsewhere (Claassen, 2005).

References

Ashurst and Hancock, 1977 K.G. Ashurst and R.D. Hancock, The thermodynamics of the formation of sulphate complexes of iron(III), cobalt(II), iron(II), manganese(II) and copper(II) in perchlorate medium, *NIM Report* **vol. 1914**, NIM, Randburg, South Africa (1977).

Babcan, 1971 J. Babcan, Synthesis of jarosite — $KFe_3(SO_4)_2(OH)_6$, *Geol. Zb.* **22** (1971) (2), pp. 299–304.

Barham, 1997 R.J. Barham, Schwertmannite, a unique mineral, contains a replaceable ligand, transforms to jarosites, hematites, and/or basic iron sulphate, *J. Mater. Res.* **12** (1997) (10), pp. 2751–2758.

Bigham et al., 1990 J.M. Bigham, U. Schwertmann, L. Carlson and E. Murad, A poorly crystallized oxyhydroxysulfate of iron formed by bacterial oxidation of Fe(II) in acid mine waters, *Geochim. Cosmochim. Acta* **54** (1990), pp. 2743–2758.

Bigham et al., 1994 J.M. Bigham, L. Carlson and E. Murad, Schwertmannite, a new iron oxyhydroxy-sulphate from Pyhasalmi, Finland, and other localities, *Min. Mag.* **58** (1994), pp. 641–648.

Bigham et al., 1996 J.M. Bigham, U. Schwertmann, S.J. Traina, R.L. Winland and M. Wolf, Schwertmannite and the chemical modeling of iron in acid surface waters, *Geochim. Cosmochim. Acta* **60** (1996), pp. 2111–2121.

Brady et al., 1986 K.S. Brady, J.M. Bigham, W.F. Jaynes and T.F. Logan, Influence of sulfate on Fe-oxide formation: comparisons with a stream receiving acid mine drainage, *Clays Clay Miner.* **34** (1986), pp. 266–274.

Claassen, 2005 Claassen, J.O., 2005. Product quality parameters in the reaction crystallization of metastable iron phases from zinc-rich solutions. PhD Thesis, University of Pretoria, Pretoria, South Africa, pp. 136.

Claassen et al., 2002 J.O. Claassen, E.H.O. Meyer, J. Rennie and R.F. Sandenbergh, Iron removal from zinc-rich process solutions: defining the Zincor Process, *Hydrometallurgy* **67** (2002), pp. 87–108.

Claassen et al., 2003 J.O. Claassen, J. Rennie, W.H. Van Niekerk, E.H.O. Meyer and R.F. Sandenbergh, Recent developments in iron removal and control at the Zinc Corporation of South Africa. In: C. Young, A. Alfantazi, C. Anderson, A. James, D. Dreisinger and B. Harris, Editors, *Hydrometallurgy 2003, 5th International Symposium Proceedings, Vancouver*, TMS Publications, Canada (2003), pp. 1675–1690.

Cornell and Schwertmann, 1996 R.M. Cornell and U. Schwertmann, *The Iron Oxides-Structure, Properties, Reactions, Occurrence and Uses*, Wiley-VCH, Weinheim, New York (1996), p. 573.

David and Klein, 2001 R. David and J. Klein, Reaction crystallization. In: A. Mersmann, Editor, *Crystallization Technology Handbook*, Marcel Dekker, New York (2001), p. 832.

Demopoulos, 1993 G. Demopoulos, Precipitation in aqueous processing of inorganic materials: a unified colloid-crystallization approach to the production of powders with controlled properties. In: H. Henein and T. Oki, Editors, *First International Conference on Processing Materials for Properties*, *The Minerals, Metals & Materials Society* (1993), pp. 537–540.

Demopoulos, 2003 G.P. Demopoulos, Short course: aqueous precipitation and crystallization for the production of particulate solids with desired properties, *Hydrometallurgy 2003, 5th International Symposium Proceedings, Vancouver, Canada, 2003* (2003).

Dirksen and Ring, 1991 J.A. Dirksen and T.A. Ring, Fundamentals of crystallization: kinetic effects on particle size distribution and morphology, *Chem. Eng. Sci.* **46** (1991) (10), pp. 2389–2427.

Garside et al., 1972 J. Garside, J. Gaska and J.W. Mullin, *J. Cryst. Growth* **13/14** (1972), p. 510.

Gösele et al., 1990 W. Gösele, W. Egel-Hess, K. Wintermantel, F.R. Faulhaber and A. Mersmann, Feststoffbildung durch fällung, *Chem. Ing. Tech.* **62** (1990), pp. 544–552.

Jambor and Dutrizac, 1998 J.L. Jambor and J.E. Dutrizac, Occurrence and constitution of natural and synthetic ferrihydrite, a widespread iron oxy-hydroxide, *Chem. Rev.* **98** (1998) (7), pp. 2549–2585.

Kind, 2002 M. Kind, Colloidal aspects of precipitation processes, *Chem. Eng. Sci.* **57** (2002), pp. 4287–4293.

Loan et al., 2001 M. Loan, G. Parkinson, M. Newman and J. Farrow, Iron oxy-hydroxide crystallization in a hydrometallurgical residue, *J. Cryst. Growth* **235** (2001), pp. 482–488.

Mersmann, 2001 A. Mersmann, Fundamentals of crystallization. In: A. Mersmann, Editor, *Crystallization Technology Handbook* (2nd edition), Marcel Dekker, New York (2001), p. 832.

Mullin, 1972 J.W. Mullin In: J.W. Mullin, Editor, *Crystallization* (2nd edition), Butterworths, London (1972).

Mullin and Ang, 1976 J.W. Mullin and N.M. Ang, *Discuss. Faraday Soc.* **61** (1976), p. 141.

Nielsen, 1964 A.E. Nielsen In: A.E. Nielsen, Editor, *Kinetics of Precipitation*, Pergamon Press, New York (1964), p. 379.

Nielsen, 1967 A.E. Nielsen In: H.S. Peiser, Editor, *Crystal Growth*, Pergamon Press, New York (1967), p. 419.

Nyvlt, 1982 J. Nyvlt In: J. Nyvlt, Editor, *Industrial Crystallization: the State of the Art* (2nd edition), Verlag Chemie, Weinheim (1982).

Nyvlt et al., 1985 J. Nyvlt, O. Söhnel, M. Matuchova and M. Broul, The Kinetics of Industrial Crystallization, *Chemical Engineering Monograph Series* **vol. 19**, Elsevier, Amsterdam (1985), p. 350.

Sakamoto et al., 1976 K. Sakamoto, M. Kanahara and K. Matsushita, Agglomeration of crystalline particles of gibbsite during the precipitation in sodium aluminate solutions, *Light Met.* **2** (1976), pp. 149–162.

Yamada, 1980 K. Yamada, Nucleation and aggregation during crystallization of aluminium tri-oxide in sodium aluminate solution, *J. Jpn. Inst. Light Met.* **32** (1980) (12), pp. 720–726.

Yakovlev et al., 1977 Y.B. Yakovlev, F.Y. Kul'ba, A.G. Pus'ko and M.N. Gerchikova, Hydrolysis of iron(III) sulphate in zinc sulphate solutions at 25, 50 and 80 °C, *Russ. J. Inorg. Chem.* **22** (1977) (1), pp. 27–29.

Corresponding author. Zincor Ltd., PO Box 218, Springs, South Africa. Tel.: +27 11 8129581; fax: +27 11 3633344.